*Desalination and Water Treatment*
www.deswater.com
doi: 10.1080/19443994.2013.810378

52 (2014) 5007–5014
July

Taylor & Francis
Taylor & Francis Group

# Degradation of dyes using combined photo-Fenton/activated carbon: synergistic effect

Niyaz Mohammad Mahmoodi*, Shooka Khorramfar

*Department of Environmental Research, Institute for Color Science and Technology, Tehran, Iran*
*Tel. +98 021 22969771; Fax: +98 021 22947537; email: mahmoodi@icrc.ac.ir*

Received 31 July 2012; Accepted 12 May 2013

ABSTRACT

In this paper, the effect of activated carbon (AC) on the photocatalytic degradation of dyes using photo-Fenton process was investigated. Reactive Red 198 (RR198) and Reactive Red 120 (RR120) were used as model dyes. The surface characteristics of AC were investigated using Fourier transform infrared. Photocatalytic dye degradation was studied using UV–Vis spectrophotometer and ion chromatography. The effects of AC dosage, initial dye concentration, pH, and salt on dye degradation were investigated. Formate, acetate, and oxalate anions were detected as dominant aliphatic intermediates, where they were further oxidized slowly to $CO_2$. Nitrate, chloride, and sulfate anions were detected as the photocatalytic mineralization products of dyes. The results indicated that the AC/Fe could be used as an eco-friendly material to remove dyes. In addition, AC has synergistic effect when degrading dyes from colored wastewater using photo-Fenton process.

*Keywords:* Synergistic effect; Photo-Fenton process; Activated carbon; Dye degradation; Colored wastewater

## 1. Introduction

The removal of dyes from wastewater is a major concern in the textile industry [1–5]. Synthetic dyes are difficult to degrade due to their complex aromatic structure. Some of them are known to be toxic [1,6]. Hence, degradation of dyes is necessary from the point of view of public health and safety.

Several methods, such as adsorption [7], nanofiltration [8], ozonation [9], electrochemical [10], etc., were used to remove dyes from wastewater.

Advanced oxidation processes (AOPs) that produce strong oxidants, such as hydroxyl radicals ($OH^\bullet$), are an emerging technique to degrade pollutants in water treatment. Hydroxyl radicals can be produced from $H_2O_2$ using homogeneous (e.g. Fenton reaction) or heterogeneous catalysts (supported metal catalysts, metal oxides, graphite, and activated carbon (AC)) [11].

The photo-Fenton process, as one of the AOPs, is widely studied. The detailed chemical mechanism of photo-Fenton is proposed [12–14]. Hydroxyl radical is produced by the cycle of oxidation and reduction reactions that requires the presence of ferrous ions ($Fe^{2+}$), hydrogen peroxide ($H_2O_2$), and UV irradiation. In the first step, ferrous ions are oxidized by $H_2O_2$, generating hydroxyl radicals. In the second step, the ferric ions ($Fe^{3+}$) are reduced photochemically to the

---

*Corresponding author.

initial oxidation state ($Fe^{2+}$) and additional hydroxyl radicals are produced [12,15–17].

In some cases, the used concentration of iron in the photo-Fenton system may exceed the limit established by environmental legislation and may require removal of ferrous or ferric ions at the end of the process.

AC is widely used as an adsorbent of pollutants due to its porous nature and large specific surface area [18–25]. Although AC adsorption method is effective for the removal of organic compounds, the AC can get easily saturated in the process which requires regeneration or complete replacement. Combining both adsorption and heterogeneous catalysis into a single process could offer an attractive alternative in the wastewater treatment.

The literature review showed that the operational parameters on dye degradation using photo-Fenton/AC were not studied in detail. In this paper, the degradation of dyes from colored textile wastewater by photo-Fenton/AC has been investigated in detail. Reactive Red 198 (RR198) and Reactive Red 120 (RR120) were used as model dyes. The surface characteristics of AC were investigated using Fourier transform infrared (FTIR). Photocatalytic dye degradation was studied using UV–Vis spectrophotometer and ion chromatography (IC). The effects of AC dosage, initial dye concentration, pH, and salt on photocatalytic dye degradation were investigated. In addition, dominant aliphatic intermediates and photocatalytic mineralization products of dyes were studied.

## 2. Experimental

Reactive Red 198 (RR198) and Reactive Red 120 (RR120) were used as model dyes. The dyes were purchased from Ciba Ltd and used without further purification. The chemical structure of the dyes is shown in Fig. 1. All other chemicals were of Analar grade and purchased from Merck (Germany).

FTIR spectroscopy (Perkin-Elmer Spectrophotometer Spectrum One) for the AC in the range of 4,000–450 $cm^{-1}$ was studied.

Experiments were carried out in a batch mode reactor (Fig. 2). The radiation source was a UV-C lamp (200–280 nm, 9 W Philips).

The dye degradation experiments were conducted by mixing AC (0.010 g for RR198 and 0.020 g for RR120) in 800 mL of dye solution (100 mg/L), $Fe^{2+}$ (2 mg/L), and $H_2O_2$ (40 mg/L) at pH 2.9 and 25˚C. The solution pH was adjusted by adding a small amount of $H_2SO_4$ or NaOH. The solution samples were withdrawn from the reaction medium at regular time intervals. The suspensions were centrifuged by Hettich EBA20 and the change in absorbance at the maximum wavelength ($\lambda_{max}$) of dyes (520 nm for RR198 and 514 nm for RR120) was monitored by UV–Vis spectrophotometer (Perkin-Elmer Lambda 25).

Ion chromatograph (METROHM 761 Compact IC) was used to assay the appearance and quantity of aliphatic carboxylic acids (formate, acetate, and oxalate) and inorganic anions formed during the degradation and mineralization of dyes using a METROSEP anion dual 2, flow 0.8 mL/min, 2 mM $NaHCO_3$/1.3 mM $Na_2CO_3$ as eluent, temperature 20˚C, pressure 3.4 MPa, and conductivity detector.

The effect of AC on photocatalytic dye degradation was investigated by contacting 800 mL of dye solution (100 mg/L), $Fe^{2+}$ (2 mg/L), and $H_2O_2$ (40 mg/L) at room temperature (25˚C) and pH 2.9 for 60 min. Different amounts of AC (0, 0.005, 0.010, 0.015, and 0.020 g) were applied.

The effect of initial dye concentration on photocatalytic dye degradation was studied. The optimum amount of AC (0.010 g for RR198 and 0.020 g for RR120) was added to 800 mL of different dye concentrations (100, 150, 200, and 250 mg/L), $Fe^{2+}$ (2 mg/L), and $H_2O_2$ (40 mg/L) at pH 2.9 for 60 min.

The effect of pH (2.9, 5, 8, and 10) on photocatalytic dye degradation was investigated by contacting 800 mL of dye solution (100 mg/L), $Fe^{2+}$ (2 mg/L), and $H_2O_2$ (40 mg/L) at room temperature (25˚C) and optimum amount of AC (0.010 g for RR198 and 0.020 g for RR120) for 60 min.

The effect of salt on photocatalytic dye degradation was studied. 0.02 mol of different salts ($Na_2SO_4$, NaCl, $Na_2CO_3$, and $NaHCO_3$) was added to 800 mL of dye solution (100 mg/L), $Fe^{2+}$ (2 mg/L), and $H_2O_2$ (40 mg/L) at room temperature (25˚C) with optimum amount of AC (0.010 g for RR198 and 0.020 g for RR120) and pH 2.9 for 60 min.

## 3. Results and discussion

### 3.1. Surface characteristics of AC

In order to investigate the surface functional groups of AC, FTIR was used (Fig. 3). The FTIR spectrum of AC shows that the peak positions are at 3,409, 2,923, 2,845, 1,600, 1,171, 1,094, and 1,042 $cm^{-1}$. The band at 3,409 $cm^{-1}$ is due to O–H and N–H stretching. The bands at 2,923 and 2,845 $cm^{-1}$ correspond to asymmetrical and symmetrical aliphatic C–H stretchings, respectively. While the band at 1,600 $cm^{-1}$ reflects C=C stretching of aromatic rings, whose intensity is enhanced by the presence of oxygen atoms as phenol or ether groups, the bands at 1,300–1,000 $cm^{-1}$ correspond to C–O stretching [26,27].

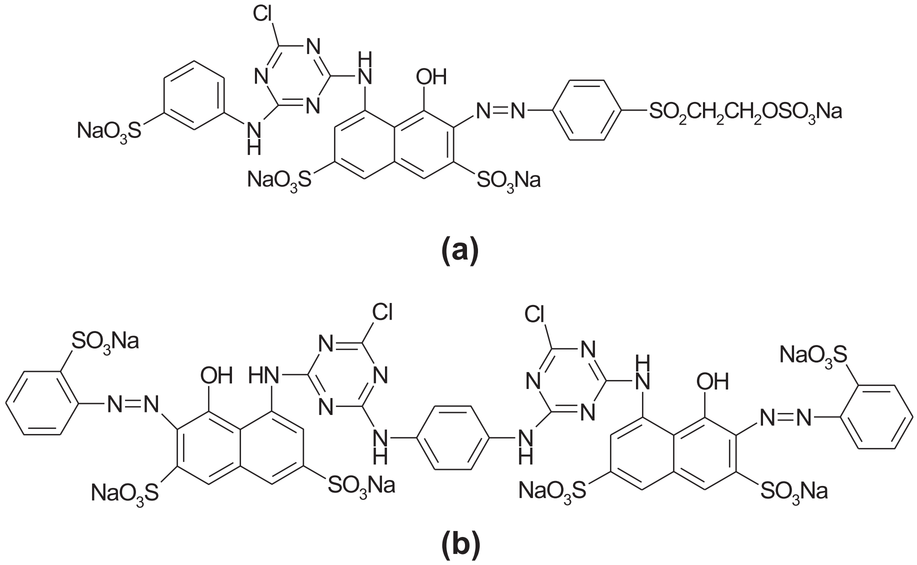

Fig. 1. The chemical structure of dyes (a) RR198 and (b) RR120.

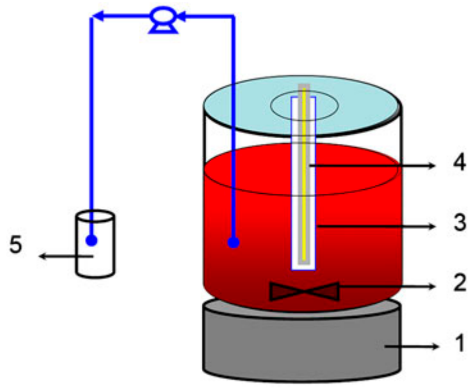

Fig. 2. Reactor (1) stirrer, (2) magnet, (3) quartz tube, (4) lamp, and (5) sample cell.

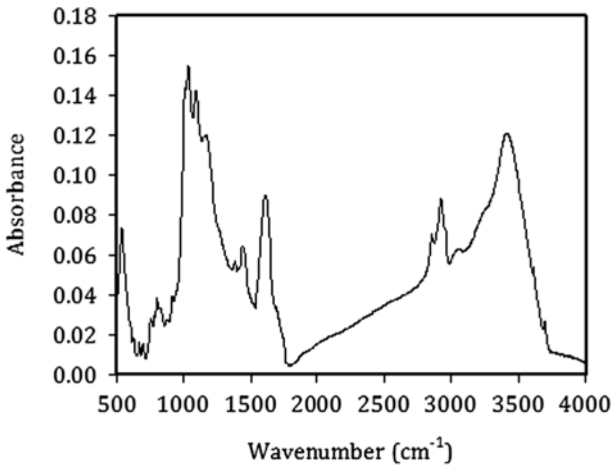

Fig. 3. FTIR spectrum of AC.

## 3.2. *Effects of operational parameters on dye oxidation*

### 3.2.1. *Effect of AC*

Adsorption of dyes on AC is a process that also presents a low performance for dye removal from solutions (1% for RR198 and 2% for RR120 after 60 min of adsorption process) because of its high molecular size and relatively low affinity to the surface of AC.

In this study, various dosages of AC were tested on dye removal by photo-Fenton process (Fig. 4). The oxidation with photo-Fenton process in the absence of AC is 73 and 71% for RR198 and RR120, respectively (Fig. 4). It was observed that the simultaneous use of

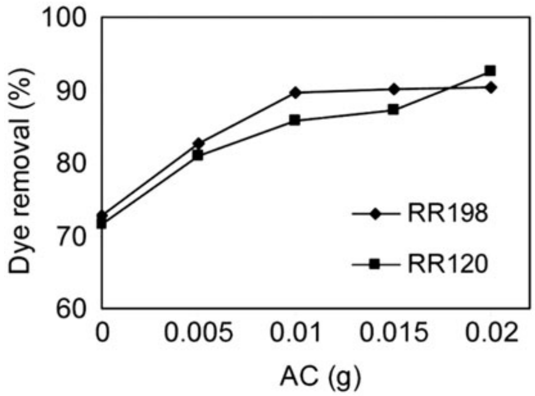

Fig. 4. The effect of AC dosage on the photocatalytic dye degradation using photo-Fenton/AC ($H_2O_2$: 8.24 mM for RR198 and 9.19 mM for RR120, Dye: 100 mg/L, $Fe^{2+}$: 2 mg/L and pH: 2.9).

AC and photo-Fenton to a certain extent yielded a significant improvement of dye degradation compared to that of the photo-Fenton alone (Fig. 4). The synergistic effect of AC on photo-Fenton was observed when the optimum AC dosage was applied (Eqs. (1)–(4)). AC catalyzes the production of free radicals, such as hydroxyl radicals, which are very active in degrading pollutants in the aqueous phase [11,28–31]. The electron transfer from the surface of AC to $Fe^{3+}$ seems to be involved in the corresponding mechanism, according to a pathway similar to the Fenton reaction (Fig. 5).

$$Fe^{2+} + H_2O_2 \rightarrow OH^{\bullet} + OH^{-} + Fe^{3+} \quad (1)$$

$$Fe^{3+} + AC \rightarrow Fe^{2+} + AC^{+} \quad (2)$$

$$AC^{+} + OH^{-} \rightarrow OH^{\bullet} + AC \quad (3)$$

$$Fe^{3+} + H_2O \rightarrow Fe^{2+} + H^{+} + OH^{\bullet} \quad (4)$$

### 3.2.2. Effect of initial dye concentration

Fig. 6 shows the dye removal using photo-Fenton/AC at different initial dye concentrations. With the increase in the dye concentration, the possible cause could be the interference from intermediates formed upon oxidation of the parental dye molecules. Such suppression would be more pronounced due to insufficiency of oxidant ($H_2O_2$) concentration and the presence of an elevated level of oxidation intermediates formed upon an increased initial dye concentration [32].

### 3.2.3. Effect of solution pH

Since dyes can be degraded at different pH values in colored effluents, comparative experiments were performed at different pH values. The pH of a solution is an important parameter in the reaction taking place on the material surface, since it influences the surface charge properties of the photocatalyst. The effect of pH on the oxidation of dyes using

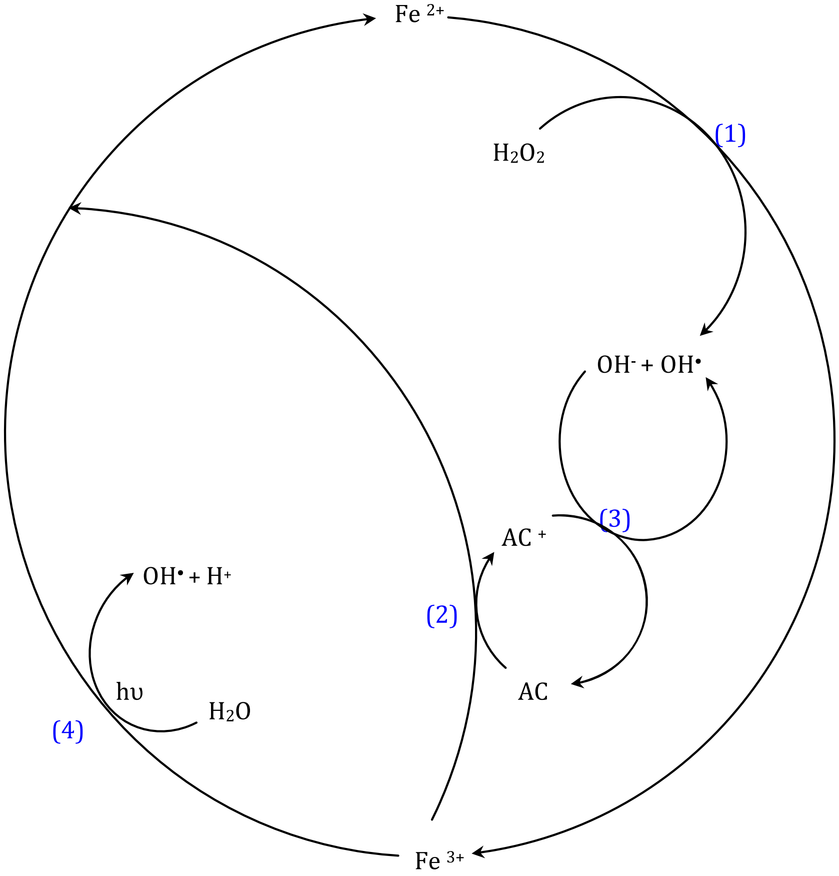

Fig. 5. The synergistic effect of AC on photo-Fenton process.

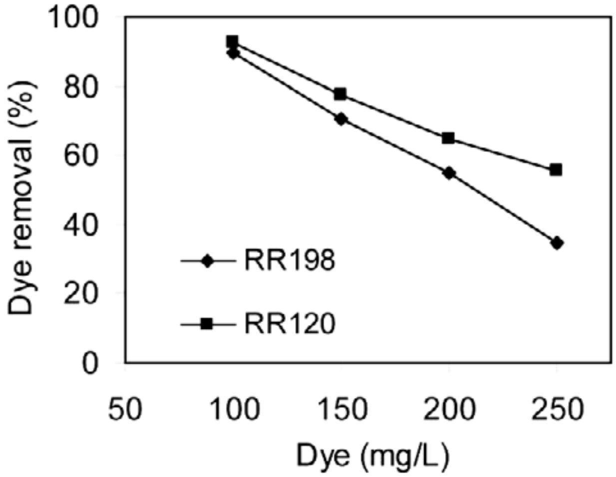

Fig. 6. The effect of dye concentration on the photocatalytic dye degradation using photo-Fenton/AC ($H_2O_2$: 8.24 mM for RR198 and 9.19 mM for RR120, $Fe^{2+}$: 2 mg/L, AC: 0.1 g/L and pH: 2.9).

photo-Fenton/AC is shown in Fig. 7. The maximum photocatalytic dye degradation is obtained at pH 2.9.

The results showed that the dye oxidation using photo-Fenton/AC increased by decrease in pH. The amount of photoregenerated Fe(II) is strongly affected by the pH-dependent hydrolytic speciation of Fe(III). At pH 2.9, Fe(III) hydroxyl complexes are highly soluble and $Fe(OH)^{2+}$, which has the highest photoreactivity, is the predominant form of the Fe(III) hydroxy complexes. For pH values above 4, the degradation strongly decreases as Fe(III) complexes precipitate and the regeneration of Fe(II) is reduced [33].

In addition, it can be attributed to the superposition of several effects such as the increase in the rate of the $H_2O_2$ decomposition (via $OOH^-$) with increasing pH, the increase in the redox potential of $H_2O_2$ (and the resulting reactive oxygen species) with decreasing pH, as well as possible changes in the chemical properties of the AC surface [5,19–21].

### 3.2.4. Effect of salt

The occurrence of dissolved inorganic ions is rather common in dyes containing industrial wastewater. These substances may compete for active sites on the AC surface or deactivate the AC and, subsequently, decrease the oxidation rate of the target dyes [32]. A major drawback resulting from the high reactivity and non-selectivity of $^{\bullet}OH$ is that it also reacts with non-target compounds present in the background water matrix, i.e. dye auxiliaries present in the dye bath. It results in higher $^{\bullet}OH$ demand to accomplish the desired degree of oxidation, or complete inhibition of advanced oxidation rate and efficiency [34].

To consider how the presence of dissolved inorganic anions affects the oxidation rate of dyes using photo-Fenton/AC, different salts, such as $Na_2SO_4$, NaCl, $Na_2CO_3$, and $NaHCO_3$, were chosen. Fig. 8 shows the effects of salts on the oxidation of dyes. The presence of these salts could inhibit $H_2O_2$ oxidation through their scavenging effects on the $OH^{\bullet}$ radicals. To generate a sufficient level of $OH^{\bullet}$ for oxidation of dyes in the presence of high levels of these anions, a higher oxidant dose should be used [8,32–35]. Carbonate and bicarbonate have buffer capacity, and so they can prevent $OH^{\bullet}$ forming. Chloride ions react with $OH^{\bullet}$ and oxidize to $Cl_2$, and decomposition mechanism of dye is ineffective.

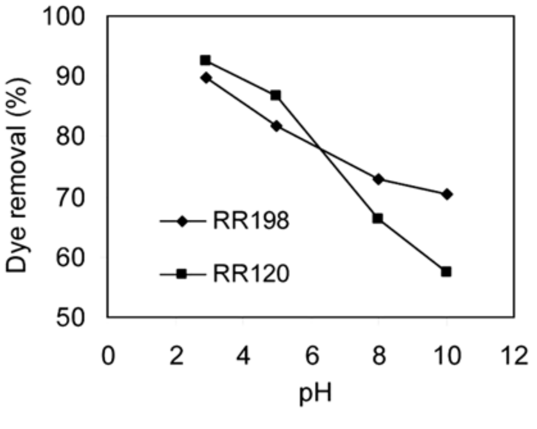

Fig. 7. The effect of pH on the photocatalytic dye degradation using photo-Fenton/AC ($H_2O_2$: 8.24 mM for RR198 and 9.19 mM for RR120, Dye: 100 mg/L, $Fe^{2+}$: 2 mg/L and AC: 0.1 g/L).

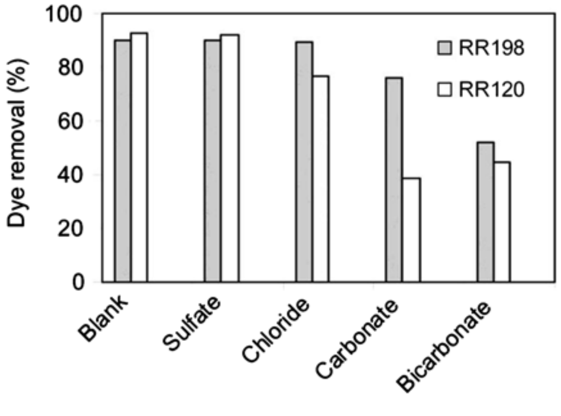

Fig. 8. The effect of salt on the photocatalytic dye degradation using photo-Fenton/AC ($H_2O_2$: 8.24 mM for RR198 and 9.19 mM for RR120, Salt: 0.02 M, Dye: 100 mg/L, $Fe^{2+}$: 2 mg/L, AC: 0.1 g/L and pH: 2.9).

### *3.3. UV–Visible spectrum studies and aromatic ring degradation*

Changes in the dyes absorptions at 250 nm ⩽ $\lambda$ ⩽ 600 nm during the oxidation at different time intervals were studied. With oxidation time elapse of 30 min, the maximum absorbance in the visible region of UV–Vis spectra decreased, which indicates that chromophores in dyes are the most active sites for oxidation attack (Fig. 9). Also, absorbance measurements of the samples at 254 nm were taken as an indication of the aromatic compound content in the solution [36]. The lack of absorbance in 254 nm after 180 min of photocatalytic degradation of RR198 and RR120 indicates the aromatic rings' destruction (Fig. 10).

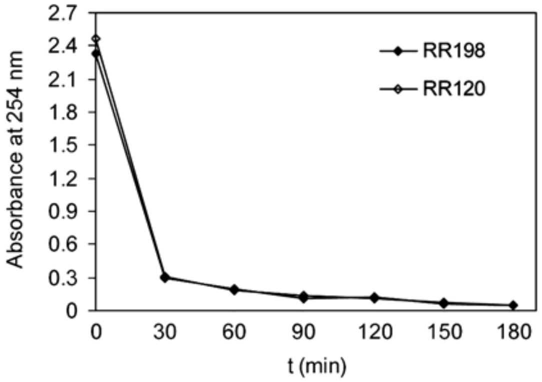

Fig. 10. Absorbance of the samples at 254 nm as an indication of the aromatic compound content during the photocatalytic dye degradation using photo-Fenton/AC ($H_2O_2$: 8.24 mM for RR198 and 9.19 mM for RR120, Dye: 100 mg/L, $Fe^{2+}$: 2 mg/L, AC: 0.1 g/L and pH: 2.9).

### *3.4. Carboxylic acid intermediates and mineralized products*

During the oxidation of dyes, various organic intermediates were produced. Consequently, destruction of the dye should be evaluated as an overall oxidation process, involving the oxidation of both the parent dye and its intermediates.

Further hydroxylation of aromatic intermediates leads to the cleavage of the aromatic ring, resulting in the formation of oxygen-containing aliphatic

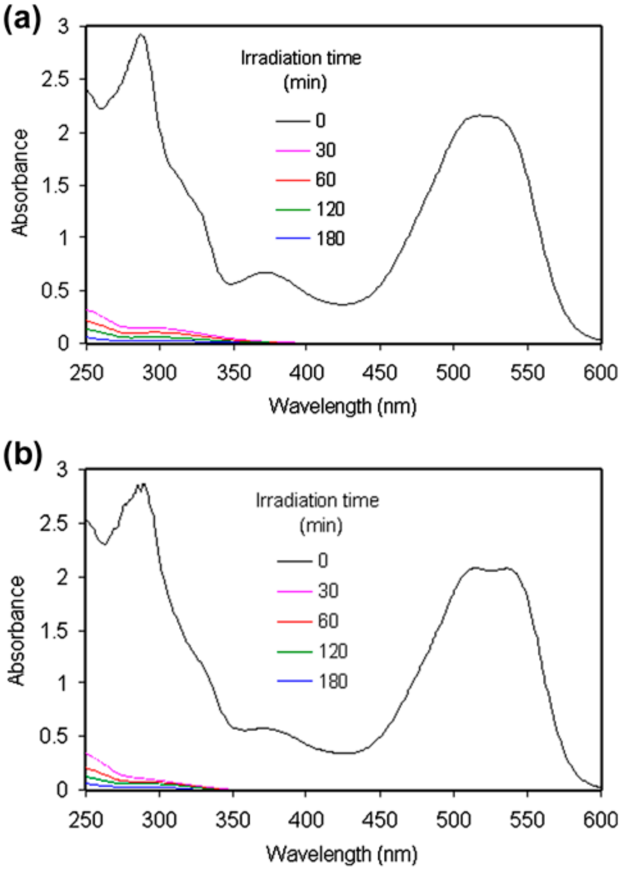

Fig. 9. The changes in UV–Vis spectra of dyes during the photocatalytic dye degradation using photo-Fenton/AC (a) RR198 and (b) RR120) ($H_2O_2$: 8.24 mM for RR198 and 9.19 mM for RR120, Dye: 100 mg/L, $Fe^{2+}$: 2 mg/L, AC: 0.1 g/L and pH: 2.9).

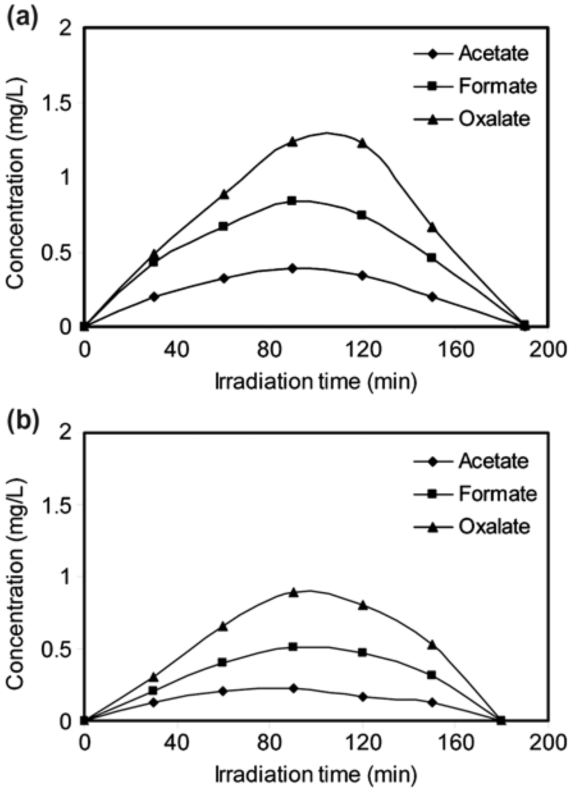

Fig. 11. Formation and disappearance of aliphatic carboxylic acids during the photocatalytic dye degradation using photo-Fenton/AC (a) RR198 and (b) RR120) ($H_2O_2$: 8.24 mM for RR198 and 9.19 mM for RR120, Dye: 100 mg/L, $Fe^{2+}$: 2 mg/L, AC: 0.1 g/L and pH: 2.9).

compounds [32]. Formate, acetate, and oxalate anions were detected as important aliphatic carboxylic acid intermediates during the oxidation of dyes (Fig. 11). Carboxylic acids can react directly with reactive species, such as hydroxyl radicals, generating $CO_2$.

Also, the photocatalytic mineralization of dye implies the appearance of inorganic products, mainly anions, since hetero-atoms are generally converted into anions in which they are at their highest oxidation degree.

The dye degradation leads to the conversion of organic carbon into harmless gaseous $CO_2$ and that of N and S heteroatoms into inorganic ions, such as nitrate and sulfate ions, respectively [1,32]. Mineralization of dyes is reported for an irradiation period of 180 min. The formation of $NO_3^-$, $SO_4^{2-}$, and $Cl^-$ from the mineralization of RR198 and RR120 was detected.

## 4. Conclusions

In this paper, the effect of AC on the degradation of dyes using photo-Fenton process was investigated. Reactive dyes were used as model dyes. The surface morphology of AC was investigated using FTIR. While selecting the optimum amount of AC dosage, the synergistic effect of AC on photo-Fenton was observed due to the catalytical performance of AC for the production of hydroxyl radicals, which are very active in oxidation reactions in the aqueous phase. Formate, acetate, and oxalate anions were detected as important aliphatic carboxylic acid intermediates during the oxidation of dyes. The formation of $NO_3^-$, $SO_4^{2-}$, and $Cl^-$ from the mineralization of RR198 and RR120 was detected. Hence, the photo-Fenton/AC technique may be a viable method for treatment of large volumes of aqueous colored dye solutions.

## References

[1] N.M. Mahmoodi, Photocatalytic ozonation of dyes using copper ferrite nanoparticle prepared by co-precipitation method, Desalination 279 (2011) 332–337.

[2] N. Atar, A. Olgun, F. Çolak, Thermodynamic, equilibrium and kinetic study of the biosorption of Basic Blue 41 using *Bacillus maceran*, Eng. Life Sci. 8 (2008) 499–506.

[3] Y. Bulut, H. Aydin, A kinetics and thermodynamics study of methylene blue adsorption on wheat shells, Desalination 194 (2006) 259–267.

[4] A. Ozcan, A.S. Ozcan, Adsorption of Acid Red 57 from aqueous solutions onto surfactant-modified sepiolite, J. Hazard. Mater. 125 (2005) 252–259.

[5] H.J. Fan, H.Y. Shu, K. Tajima, Decolorization of acid black 24 by the FeGAC/$H_2O_2$ process, J. Hazard. Mater. 128 (2006) 192–200.

[6] V.P. Santos, M.F.R. Pereira, P.C.C. Faria, J.J.M. Orfao, Decolourisation of dye solutions by oxidation with $H_2O_2$ in the presence of modified activated carbons, J. Hazard. Mater. 162 (2009) 736–742.

[7] N.M. Mahmoodi, F. Najafi, A. Neshat, Poly (amidoamine-co-acrylic acid) copolymer as a polymeric adsorbent: Synthesis, characterization, and its dye removal ability, Ind. Crops Prod. 42 (2013) 119–125.

[8] N.M. Mahmoodi, F. Najafi, Preparation of surface modified zinc oxide nanoparticle with high capacity dye removal ability, Mater. Res. Bull. 47 (2012) 1800–1809.

[9] N.M. Mahmoodi, F. Najafi, Synthesis, amine functionaliztion and dye removal ability of titania/silica nano-hybrid, Microporous Mesoporous Mater. 156 (2012) 153–160.

[10] N.M. Mahmoodi, Equilibrium, kinetic and thermodynamic of dye removal using alginate from binary system, J. Chem. Eng. Data 56 (2011) 2802–2811.

[11] T.A. Kurniawan, W.H. Lo, Removal of refractory compounds from stabilized landfill leachate using an integrated $H_2O_2$ oxidation and granular activated carbon (GAC) adsorption treatment, Water Res. 43 (2009) 4079–4091.

[12] J.F. Moraes, D.N. Silva, F.H. Quina, O. Chiavone-Filho, C.A. O. Nascimento, Utilization of solar energy in the photodegradation of gasoline in water and of oil-field-produced water, Environ. Sci. Technol. 38 (2004) 3746–3751.

[13] J.J. Pignatello, Dark and photoassisted $Fe^{3+}$-catalyzed degradation of chlorophenoxy herbicides by hydrogen peroxide, Environ. Sci. Technol. 26 (1992) 944–951.

[14] S.H. Bossmann, E. Oliveros, S. Gob, S. Siegwart, E.P. Dahlen, L. Payawan, M. Straub, M. Woner, A.M. Braun, New evidence against hydroxyl radicals as reactive intermediates in the thermal and photochemically enhanced Fenton reactions, Phys. Chem. 102 (1998) 5542–5550.

[15] T. Krutzler, H. Fallmann, P. Maletzky, R. Bauer, S. Malato, J. Blanco, Solar driven degradation of 4-chlorophenol, Catal. Today 54 (1999) 321–327.

[16] S.M. Kim, A. Vogelpohl, Degradation of organic pollutants by the photo-Fenton process, Chem. Eng. Technol. 21 (1998) 187–191.

[17] T. Krutzler, R. Bauer, Optimization of photo-Fenton prototypereactor, Chemosphere 38 (1999) 2517–2532.

[18] F. Rodriguez-Reinoso, The role of carbon materials in heterogeneous catalysis, Carbon 36 (1998) 159–175.

[19] G. Yu, S. Lu, H. Chen, Z. Zhu, Diesel fuel desulfurization with hydrogen peroxide promoted by formic acid and catalyzed by activated carbon, Carbon 43 (2005) 2285–2294.

[20] G. Yu, S. Lu, H. Chen, Z. Zhu, Oxidative desulfurization of diesel fuels with hydrogen peroxide in the presence of activated carbon and formic acid, Energy Fuels 19 (2005) 447–452.

[21] A. Georgi, F.D. Kopinke, Interaction of adsorption and catalytic reactions in water decontamination processes: Part I. Oxidation of organic contaminants with hydrogen peroxide catalyzed by activated carbon, Appl. Catal., B 58 (2005) 9–18.

[22] A.R. Yeddou, B. Nadjemi, F. Halet, A. Ould-Dris, R. Capart, Removal of cyanide in aqueous solution by oxidation with hydrogen peroxide in presence of activated carbon prepared from olive stones, Miner. Eng. 23 (2010) 32–39.

[23] S.A. El-molla, G.A. El-shobaky, S.A.S. Ahmed, Catalytic promotion of activated carbon by treatment with some transition metal cations, Chin. J. Catal. 28 (2007) 611–616.

[24] P.C.C. Faria, J.J.M. Orfao, M.F.R. Pereira, Mineralisation of coloured aqueous solutions by ozonation in the presence of activated carbon, Water Res. 39 (2005) 1461–1470.

[25] H.H. Huang, M.C. Lu, J.N. Chen, C.T. Lee, Catalytic decomposition of hydrogen peroxide and 4-chlorophenol in the presence of modified activated carbons, Chemosphere 51 (2003) 935–943.

[26] J. He, W. Ma, J. He, J. Zhao, J.C. Yu, Photooxidation of azo dye in aqueous dispersions of $H_2O_2$/FeOOH, Appl. Catal. B 39 (2002) 211–220.

[27] D.L. Pavia, G.M. Lampman, G.S. Kaiz, Introduction to Spectroscopy: A guide for Students of Organic Chemistry, WB. Saunders, Philadelphia, 1987.

[28] A. Bach, R. Semiat, The role of activated carbon as a catalyst in GAC/iron oxide/$H_2O_2$ oxidation process, Desalination 273 (2011) 57–63.

[29] N.A. Klimenko, L.A. Savchina, T.V. Polyakova, I.P. Kozyatnik, Adsorption—catalytic removal of fulvic acids on activated carbons in the presence of hydrogen peroxide, J. Water Chem. Technol. 31 (2009) 92–97.

[30] L.C.A. Oliveira, C.N. Silva, M.I. Yoshida, R.M. Lago, The effect of $H_2$ treatment on the activity of activated carbon for the oxidation of organic contaminants in water and the $H_2O_2$ decomposition, Carbon 42 (2004) 2279–2284.

[31] F. Lucking, H. Koser, M. Jank, A. Ritter, Iron powder, graphite and activated carbon as catalysts for the oxidation of 4-chlorophenol with hydrogen peroxide in aqueous solution, Water Res. 32 (1998) 2607–2614.

[32] I.K. Konstantinou, T.A. Albanis, $TiO_2$-assisted photocatalytic degradation of azo dyes in aqueous solution: Kinetic and mechanistic investigations—A review, Appl. Catal. B 49 (2004) 1–14.

[33] S.M. Kim, A. Vogelpohl, Degradation of organic pollutants by the photo-Fenton-process, Chem. Eng. Technol. 21 (1998) 187–191.

[34] I. Arsalan-Alaton, A review of the effects of dye-assisting chemicals on advanced oxidation of reactive dyes in wastewater, Color. Technol. 119 (2003) 345–353.

[35] S.S. Lin, M.B. Gurol, Catalytic decomposition of hydrogen peroxide on iron oxide: Kinetics, mechanism and implications, Environ. Sci. Technol. 32 (1998) 1417–1423.

[36] D. Georgiou, P. Melidis, A. Aivasidis, K. Gimouhopoulos, Degradation of azo reactive dyes by ultraviolet radiation in the presence of hydrogen peroxide, Dyes Pigm. 52 (2002) 69–78.